Ionics (2017) 23:1309–1317
DOI 10.1007/s11581-016-1944-2

ORIGINAL PAPER

Simple non-enzymatic electrochemical sensor for hydrogen peroxide based on nafion/platinum nanoparticles/reduced graphene oxide nanocomposite modified glassy carbon electrode

Cong Zhang[1] · Haohai Jiang[2] · Rui Ma[1] · Yanyan Zhang[1] · Qiang Chen[1]

Received: 9 August 2016 / Revised: 4 December 2016 / Accepted: 18 December 2016 / Published online: 3 January 2017

Abstract A facile and effective strategy to fabricate non-enzymatic H_2O_2 sensor was developed based on Nafion/Platinum nanoparticles/reduced graphene oxide (Nafion/Pt NPs/RGO) nanocomposite modified glassy carbon (GC) electrode. The morphology of Nafion/Pt NPs/RGO nanocomposite was characterized by transmission electron microscopy (TEM), energy-dispersive X-ray spectroscopy (EDX) analyzer, Fourier transform infrared spectrum (FT-IR), and X-ray diffraction (XRD) spectrum respectively. The electrochemical properties of the prepared H_2O_2 sensor were evaluated by cyclic voltammetry and chronoamperometry. The prepared H_2O_2 sensor exhibited excellent electroreduction activity toward H_2O_2 with a wide linear range of 0.005–3 mM, a remarkable sensitivity of 132.8 μA mM^{-1} cm^{-2}, and a low detection limit of 0.4 μM (S/N = 3). In addition, it showed good selectivity, reproducibility, and long-term stability. The excellent performance of the sensor might be attributed to the synergic effect of nanohybrids. These favorable results indicated that the prepared Nafion/Pt NPs/RGO nanocomposite is promising for fabricating non-enzymatic H_2O_2 sensor.

Keywords Graphene · Pt nanoparticles · Nafion · Non-enzymatic · Hydrogen peroxide sensor

Introduction

Hydrogen peroxide (H_2O_2) is an essential intermediate in environmental and biological reactions. It is very important to reliable and fast determination of H_2O_2 in many areas such as medicine, food control, and industrial and environmental analysis [1, 2]. Hence, the study of reliable and fast determination of H_2O_2 has attracted extensive attention. Many analytical techniques have been developed for the determination of H_2O_2 such as fluorescence [3], chemiluminescence [4], spectrophotometry [5], high-performance liquid chromatography [6], electrochemical approaches [7, 8], etc. Because of the redox behavior of H_2O_2, the electrochemical method has received a significant interest in the determination of H_2O_2 over other techniques due to its simplicity, high sensitivity, selectivity, and compatibility toward miniaturization [9]. Among the electrochemical H_2O_2 sensors, the enzyme-modified electrodes are frequently used to detect H_2O_2 with satisfactory sensitivity. However, the enzyme-modified sensors have some inevitable drawbacks such as the complex fabrication procedure, limited lifetime, stability problem, and high cost of the enzymes. Thus, many efforts have been devoted to the non-enzymatic H_2O_2 sensors based on functional nanocomposites [10–12]. The development of a high sensitivity and good selectivity catalyst for non-enzymatic H_2O_2 detection is still highly desirable in this field.

Graphene, a monolayer of carbon atoms closely packed into honeycomb two-dimensional carbon material, has received considerable attentions, owing to its large surface-to-volume ratio, high electrical conductivity, chemical stability, and excellent electronic properties [13–16]. In

Cong Zhang and Haohai Jiang contributed equally to this work.

Electronic supplementary material The online version of this article (doi:10.1007/s11581-016-1944-2) contains supplementary material, which is available to authorized users.

✉ Qiang Chen
qiangchen@nankai.edu.cn

[1] The Key Laboratory of Bioactive Materials, Ministry of Education, College of Life Science, Nankai University, Weijin Road No. 94, Tianjin 300071, People's Republic of China

[2] North China Pharmaceutical Co., Ltd, Shijiazhuang 052160, People's Republic of China

electrochemical sensing, graphene has been particularly used as an electrode material, owing to its excellent electrical conductivity, high electron transfer rate, and enormous electroactive area. Graphene is usually obtained by various techniques, such as mechanical exfoliation, chemical vapor deposition, epitaxial growth, and liquid phase exfoliation [17, 18]. Among these techniques, the chemical reduction of graphene oxide (GO) is an effective method for preparing graphene [19]. Moreover, it is also a facile and effective strategy to fabricate graphene-based materials because of simplicity, low cost, and easy scale up. However, graphene agglomerates easily due to Van der Waals force, which limits its application [20]. Thus, it is necessary to select suitable biopolymers to improve the dispersion of graphene in aqueous solution.

Nafion, composed of mainly hydrophobic backbone ($-CF_2$ groups) and hydrophilic chains ($-SO_3^-$ groups), has been comprehensively employed as an electrode modifier agent with excellent properties such as its antifouling capacity, chemical inertness, and high permeability to cations [21]. Furthermore, it is easy to functionalize carbon nanomaterials based on supramolecular assembly by adding Nafion into alcoholic solutions of carbon nanomaterials [22]. Nafion could effectively improve the hydrophilicity and solubility of graphene in aqueous solution [23]. The perfluorocarbon chains in Nafion could maintain the hydrophobicity of graphene and improve its dispersity. Also, the sulphonic groups could prevent the stacking of graphene layers [24].

Recently, graphene-based materials have been deeply investigated as novel electrode modification materials for the improvement of sensing sensitivity because of π–π stacking and synergetic effects with other materials. Recently, platinum nanoparticles (Pt NPs) have been attached an enormous amount of interests for their high electron transfer rate and excellent electrocatalytic activities toward H_2O_2 [25–27]. What's more, Pt NPs exhibit the property of validly lessening the oxidation/reduction overvoltage in the electrochemical detection of H_2O_2, which can effectively avoid the interference from other co-existing substances [28]. Hence, it has become very popular in using Pt nanomaterials to fabricate H_2O_2 sensors. Furthermore, the introduction of metal nanoparticles into the dispersion of graphene sheets can inhibit the aggregation of graphene sheets, result in mechanically jammed, and exfoliate graphene agglomerate with very high surface area [29].

The aim of this work is to develop a facile and effective strategy to fabricate non-enzymatic H_2O_2 electrochemical sensor. Nafion/Pt NPs/RGO nanocomposite was prepared by a facile, eco-friendly, and controllable route. Since Nafion is composed of mainly hydrophobic and hydrophilic chains, it was used to effectively disperse RGO/Pt NPs hybrids in aqueous solution and to enhance the stability of the modified electrodes. A novel non-enzymatic electrochemical sensor for direct analytical detection of H_2O_2 was successfully papered based on Nafion/Pt NPs/RGO nanocomposite modified glassy carbon electrode. The electrochemical properties were evaluated by cyclic voltammetry and chronoamperometry. The resulting electrode showed excellent electrocatalytic activity toward H_2O_2.

Experimental

Reagents and materials

Graphene oxide (GO) was purchased from Nanjing XFNANO Materials Tech Co. Potassium Hexachloroplatinate (K_2PtCl_6), and Nafion was obtained from Sigma-Aldrich Co. Sodium borohydride ($NaBH_4$) and hydrogen peroxide (H_2O_2, 30%, *v*/*v* aqueous solution) were purchased from Tianjin Chemical Factory (China). Freshly prepared 0.1 M phosphate buffer solution, consisting of Na_2HPO_4 and NaH_2PO_4, was used as the supporting electrolyte. Na_2HPO_4 and NaH_2PO_4 were purchased from Tianjin Damao Chemical Reagent Co. (China). All aqueous solutions were prepared with doubly distilled water.

Apparatus

Electrochemical experiments were performed on a 283 Potentiostat-Galvanostat electrochemical workstation (EG&G PARC with M 270 software) with a conventional three-electrode system with the modified electrode as the working electrode, an Ag/AgCl electrode (saturated with KCl) as the reference electrode, and a platinum wire (1 mm diameter) as the counter electrode.

Nanocomposites were characterized by transmission electron microscopy (TEM, Tecnai G^2 F 20 instrument, Philips Holland), energy-dispersive X-ray spectroscopy analyzer (EDX, which was equipped on the Tecnai G^2 F 20 instrument), Fourier transform infrared spectrum (FT-IR, TENSOR 37, Bruker, German), and X-ray diffraction analysis (XRD, Rigaku, Japan).

Preparation of Nafion/Pt NPs/RGO

A total of 20 mg of GO and 20 mL of doubly distilled water were mixed through sonication for 2 h to obtain GO suspension solution (1 mg/mL). Subsequently, 10 μL of K_2PtCl_6 solution (6 mM) was added to GO suspension with sonication for 30 min. Afterwards, fresh $NaBH_4$ solution was added dropwise into the above suspension solution and kept stirring at room temperature for 24 h. Finally, Pt NPs/RGO was obtained through centrifugation and washed several times. Afterwards, the products were dried and resuspended in doubly distilled water at 1 mg/mL. Finally, 1 mL Nafion alcohol

solution (5 wt%) was added with sonication for 1 h to obtain Nafion/Pt NPs/RGO suspension solution.

Preparation of modified electrodes

Prior to experiment, the GC electrode was polished with 0.3 and 0.05 μm α-alumina powder sequentially, followed by ultrasonically cleaning in doubly distilled water and ethanol for 5 min, respectively. Afterwards, 6 μL of Nafion/Pt NPs/RGO suspension solution was immobilized on the surface of the GC electrode and dried naturally. The Nafion/Pt NPs/RGO modified GC electrode was directly used as a non-enzymatic H_2O_2 sensor for the determination of H_2O_2.

Results and discussion

Characterization of Nafion/Pt NPs/RGO

Figure 1 shows the typical TEM images of the Nafion/RGO and Nafion/Pt NPs/RGO. As shown in Fig. 1a and Fig. S1, a typical wrinkled RGO sheet (Fig. S1) can be seen, and RGO sheets were compactly coated by polymer and exfoliated completely by Nafion (Fig. 1a). As shown in Fig. 1b, Pt NPs were well scattered on the surface of RGO sheet with very few aggregation, indicating that RGO made an outstanding contribution to promoting the uniform distribution of Pt NPs. Highly dispersed Pt NPs on RGO supports with larger surface

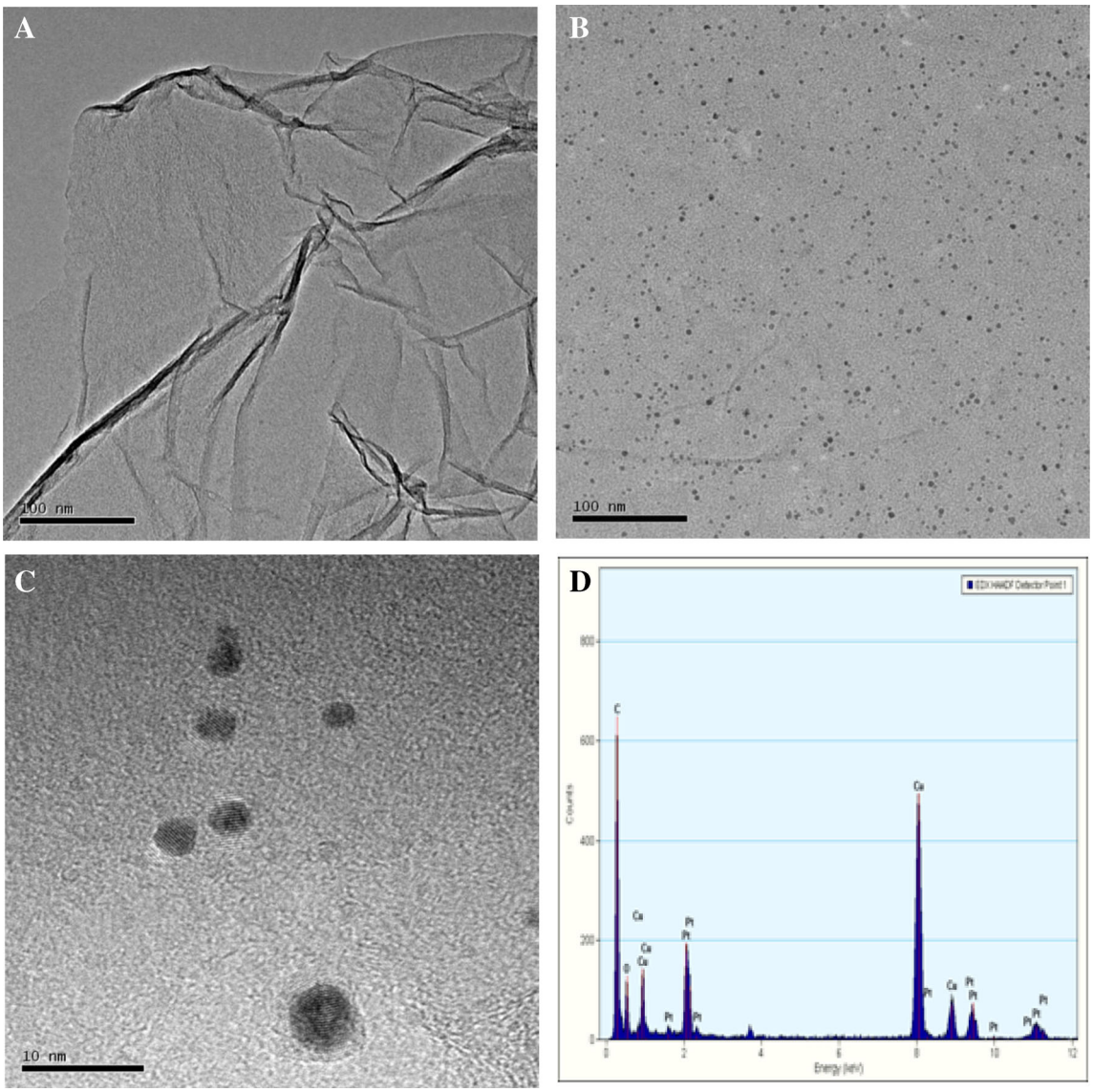

Fig. 1 TEM images of the Nafion/RGO (**a**) and Nafion/Pt NPs/RGO under different magnification (**b** and **c**); EDX spectrum of Pt NPs/RGO nanocomposite (**d**)

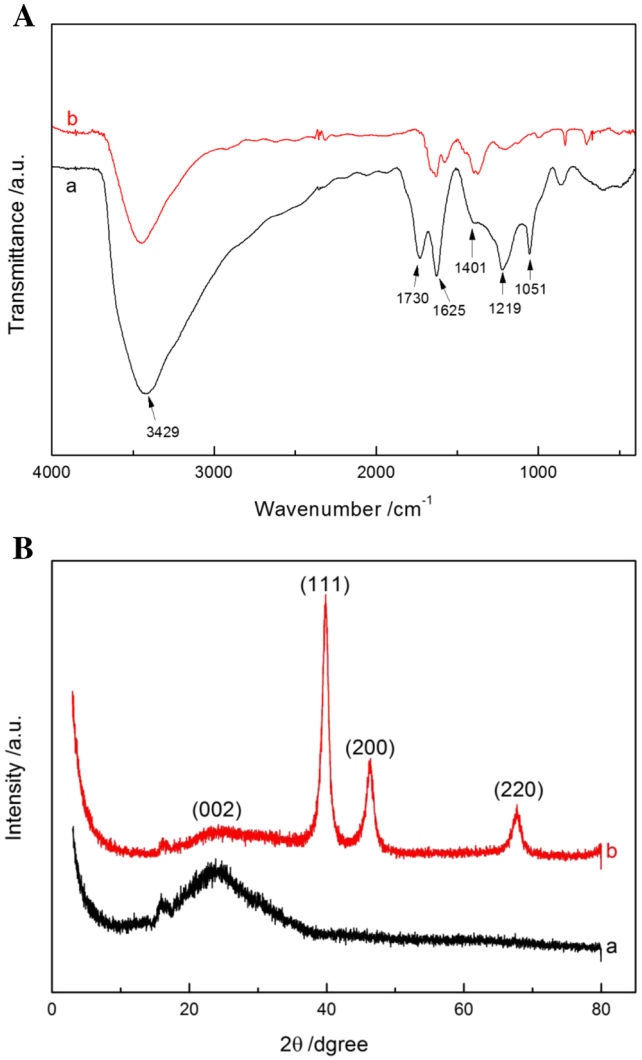

Fig. 2 **a** FT-IR spectra of GO (*a*) and RGO/Pt NPs (*b*). **b** XRD patterns of Nafion/RGO (*a*) and Nafion/Pt NPs/RGO/GC (*b*)

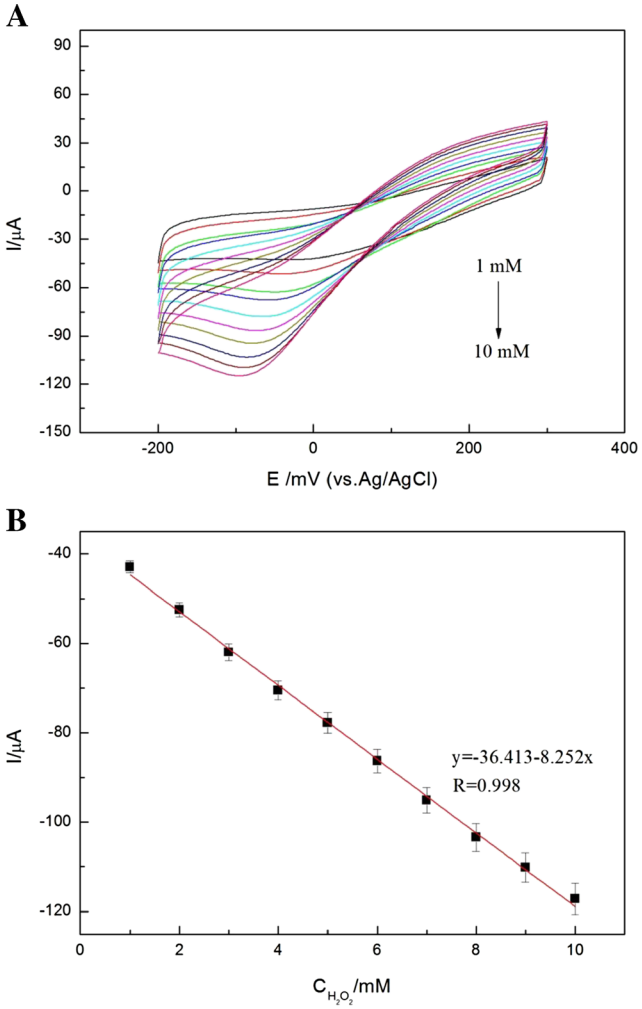

Fig. 4 **a** CVs of Nafion/Pt NPs/RGO/GC electrode in 0.1 M PBS (pH 7.0) at the scan rate 50 mV s^{-1} with different concentrations of H_2O_2 (from 1 to 10 mM). **b** The plot of the cathodic peak current values against the concentration

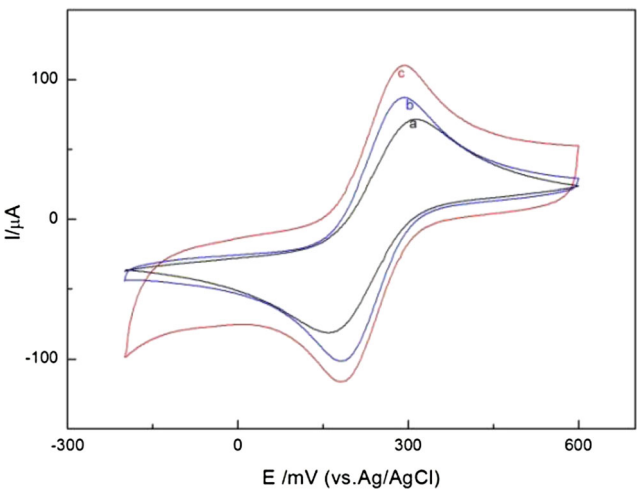

Fig. 3 CVs of bare GCE (a), Nafion/RGO/GC electrode (b), and Nafion/Pt NPs/RGO/GC electrode (c) recorded in 0.1 M KCl solution containing 10 mM $[Fe(CN)_6]^{3-}$. Scan rate: 50 mV s^{-1}

areas have many advantages in catalytic activity and sensor sensitivity [30]. The lattice structure of Pt NPs could be observed clearly under the high magnification. As shown in Fig. 1d, the EDX analysis further revealed that the nanocomposite was consisted of C, O, and Pt elements, and the Cu element in the spectrum should be from the substrate, which confirmed that Pt NPs had been coated on the RGO sheets.

FT-IR spectra further clarify the successful synthesis of Pt NPs/RGO. As shown in Fig. 2a (curve a), some peaks at 3429, 1730, 1625, 1401, 1219, and 1051 cm^{-1} can be seen, owing to O–H stretching vibration, carbonyl C═O stretching, aromatic C═C stretching, C–OH stretching, C–O–C stretching, and alkoxy C–O stretching [31]. However, in curve b of Pt NPs/RGO, the peak intensities at 3429, 1219, and 1055 cm^{-1}

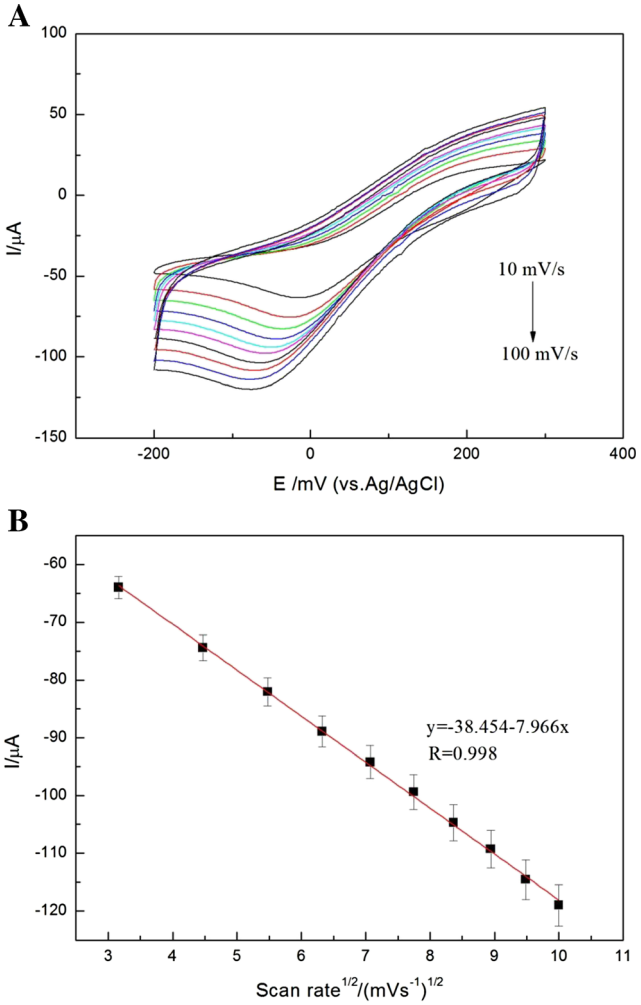

Fig. 5 **a** CVs of the Nafion/Pt NPs/RGO/GC electrode 0.1 M PBS (pH 7.0) with 5 mM H_2O_2 at different scan rate: 10, 20, 30, 40, 50, 60, 70, 80, 90, and 100 mV s^{-1}. **b** The plot of the cathodic peak current values against the scan rate

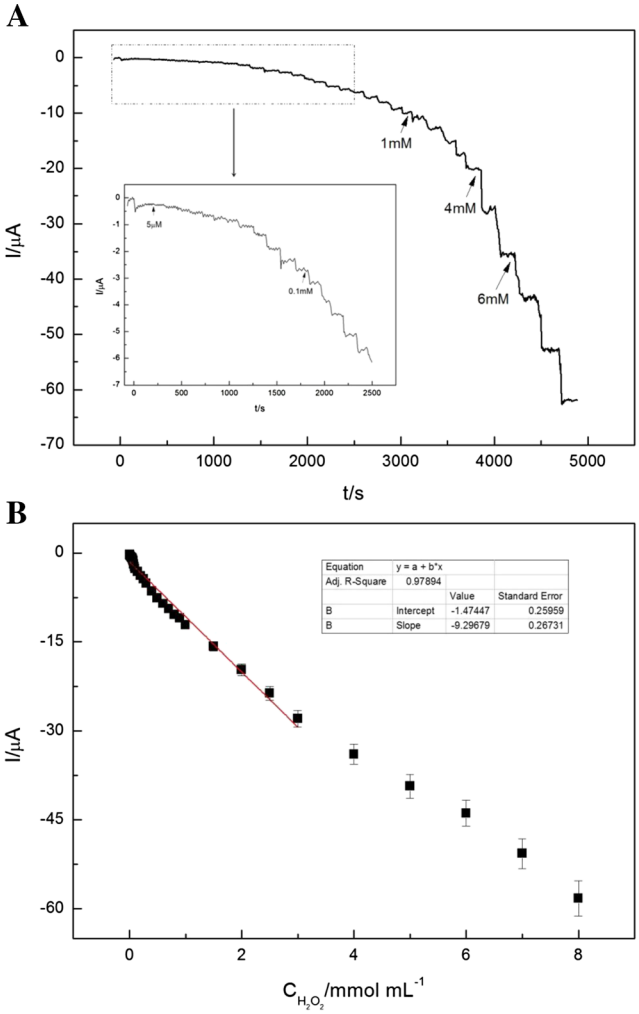

Fig. 6 **a** Amperometric response of Nafion/Pt NPs/RGO/GC electrode upon successive additions of H_2O_2 into 0.1 M PBS solution under stirring. The *inset* was the amplification of curve with the lower concentration region, Scan rate: 50 mV s^{-1}. **b** The calibration curve between amperometric response and H_2O_2 concentration

dramatically decreased after the reduction of GO. These intensities markedly decreased or even disappeared, confirming the successful reduction of GO to RGO [32]. The typical C═O absorption bands at 1730 cm^{-1} almost disappeared, indicating that the carbonyl groups on the surface of GO sheets were modified by Pt NPs. This result further confirmed that Pt NPs/RGO nanocomposite had been synthesized successfully.

Figure 2b exhibits the XRD pattern of Nafion/RGO (curve a) and Nafion/Pt NPs/RGO (curve b). A characteristic diffraction peak at 16.9° was assigned to the Nafion [23, 33], and the peak at 23.99° (002) was the typical diffraction peak of RGO, owing to the reduction of GO [34], which indicated that Nafion/RGO was successfully acquired. In curve b, the strong peaks at 39.8°, 46.3°, and 67.8° were attributed to the characteristic (111), (200), and (220) crystals of the Pt [35, 36]. Moreover, the characteristic diffraction peaks of Nafion and RGO were also observed, indicating that Nafion/Pt NPs/RGO nanocomposite had been successfully prepared.

Electrochemical characterization of Nafion/Pt NPs/RGO/GC electrode

Cyclic voltammetry (CV) of bare GC electrode (a), Nafion/RGO/GC electrode (b), and Nafion/Pt NPs/RGO/GC electrode (c) recorded in 0.1 M KCl solution containing 10 mM $[Fe(CN)_6]^{3-}$ are shown in Fig. 3. As shown in curve c, there are a couple of well-defined redox peaks of Nafion/Pt NPs/RGO/GC electrode at 290 and 190 mV, indicating Nafion/Pt NPs/RGO/GC electrode has a fast electron transfer rate. By the calculation, the electroactive surface area of Nafion/Pt NPs/

Table 1 Comparison of Pt-based electrodes response to H_2O_2

Electrode	Sensitivity ($\mu A\ mM^{-1}\ cm^{-2}$)	LOD (μM)	linear range (μM)	Reference
PVA-MWCNTs-PtNPs	122.63	0.7	2–3800	[28]
Pt-PPy-GC	80.4	1.2	1000–8000	[38]
PtPNW@C nanoparticles	6.28	0.002	0.01–1.2	[39]
PtNP-TiO_2	1.68	4	4–1250	[40]
Pt/rGO–CNT paper NPs	1.41	0.01	0.1~25	[41]
Graphene-Pt nanocomposite	–	0.5	2~710	[42]
Pt NP-PAni	96.1	0.7	10–8000	[43]
Pt-DENs/GOx/Pt-DENs/PAni/PSS	39.63	0.5	10–4500	[44]
Nafion/Pt NPs/RGO	132.8	0.4	5–3000	This work

RGO/GC electrode was about 1.26 and 1.55 times higher than those of Nafion/RGO/GC electrode and bare GC electrode, respectively, according to the Randles-Sevcik eq. [37]:

$$I_p = 2.69 \times 10^5 A D^{1/2} n^{3/2} v^{1/2} C \quad (1)$$

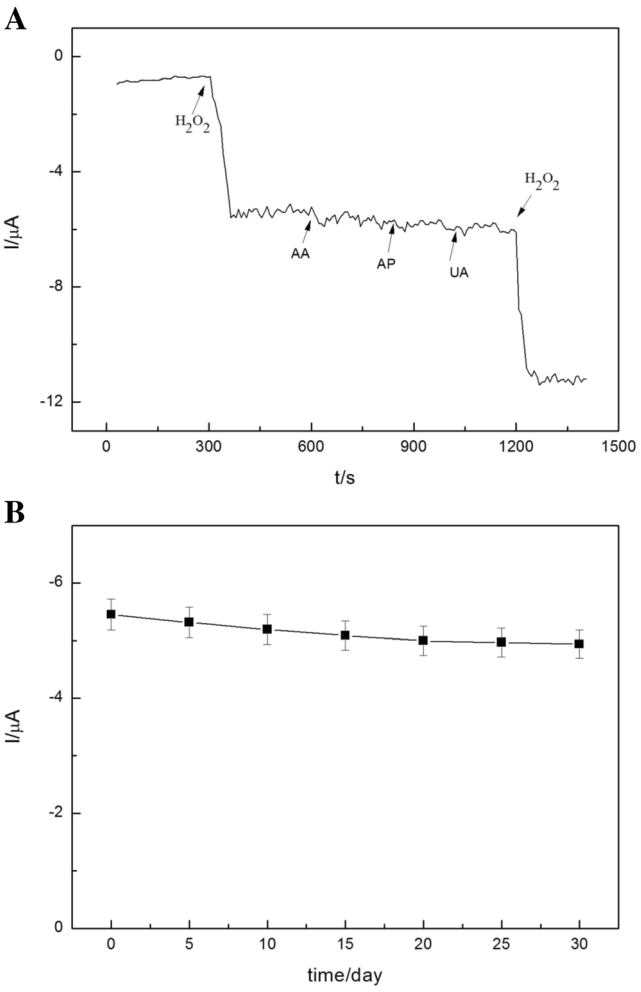

Fig. 7 **a** Amperometric response of Nafion/Pt NPs/RGO/GC electrode upon successive addition of 0.5 mM H_2O_2, 0.1 mM ascorbic acid (AA), 0.1 mM acetaminophen (AP) 0.1 mM uric acid (UA) and 0.5 mM H_2O_2. **b** The long-term stability of the non-enzymatic H_2O_2 sensor

Where I_p represents the redox peak current, A is the electrode's electroactive surface area, D is the diffusion coefficient of the molecule in solution which is $(6.70 \pm 0.02) \times 10^{-6}\ cm^2\ s^{-1}$, n is the number of electron participating in the reaction which is equal to 1, v is the scan rate ($V\ s^{-1}$), and C is the concentration of the probe molecule in the solution. These excellent results indicate that the prepared Nafion/Pt NPs/RGO nanocomposite is undeniably suitable as an electron transfer mediator between $[Fe(CN)_6]^{3-}$ and the GC electrode, which should be attributed to the large edge plane/basal plane ration and high electrical conductivity of RGO and Pt NPs. Moreover, there may be a synergistic effect between RGO and Pt NPs, which can facilitate the electronic transfer.

Cyclic voltammetric behavior of Nafion/Pt NPs/RGO/GC electrode to H_2O_2

Figure 4a shows the CVs of Nafion/Pt NPs/RGO/GC electrode in 0.1 M PBS (pH 7.0) at the scan rate 50 mV s^{-1} with different concentrations of H_2O_2 (from 1 to 10 mM). It can be seen that the cathodic peak current gradually increased with the increase of H_2O_2 concentration. As shown in Fig. 4b, the cathodic peak current was linearly proportional to the concentration of H_2O_2 ($R^2 = 0.998$), indicating that it was possible to construct an electrochemical sensor which would behave well in the amperometric experiments.

CVs of Nafion/Pt NPs/RGO/GC electrode in 0.1 M PBS (pH 7.0) containing 5 mM H_2O_2 with varying the scan rates are shown in Fig. 5a. It can been found that the cathodic peak current increased as the scan rate increased from 10 to 100 mV s^{-1}, while the cathodic peak potential shifted to a

more negative region. As shown in Fig. 5b, there was a good linearity between the cathodic peak current and the scan rate (R^2 = 0.998), indicating the electrochemical process was diffusion controlled.

Amperometric response of Nafion/Pt NPs/RGO/GC electrode to H_2O_2

Amperometric responses of Nafion/Pt NPs/RGO/GC electrode upon successive addition of H_2O_2 into 0.1 M PBS under optimum conditions (Optimization of experimental parameter is presented in Supplementary material) are shown in Fig. 6a. It can be clearly seen that the Nafion/Pt NPs/RGO/GC electrode showed a rapid and stable response to the addition of H_2O_2, and the time of current response before it reached 95% of steady-state current was less than 6 s. The calibration curves are shown in Fig. 6b, and the regression equation is $y = -1.474–9.297\times$ (R = 0.979). We found that the prepared non-enzymatic H_2O_2 sensor exhibited wide linear range from 0.005 to 3 mM with remarkable sensitivity of 132.8 μA mM^{-1} cm^{-2}, and the detection limit was calculated from 3× blank variance/slope found to be 0.4 μM at the signal-to-noise ratio of 3. In Table 1, we also compared the characteristics of the prepared non-enzymatic sensor with other relevant sensors collected from the literature. It can be seen that the performances of the Nafion/Pt NPs/RGO/GC electrode were obviously better than previously reported sensors. These excellent performances further revealed that Nafion/Pt NPs/RGO nanocomposites are promising modified electrode materials in H_2O_2 detection. These excellent performances of the Nafion/Pt NPs/RGO/GC electrode may be attributed to the synergistic effect between RGO and Pt NPs, which promotes large amount of H_2O_2 adsorbing on the electrode surface, accelerates the electron transfer rate between the surface of GC electrode and H_2O_2, and increases the electrocatalytic active area.

Selectivity, reproducibility, and stability of the modified electrode

The selectivity was studied by comparing the amperometric responses to successive addition of 0.5 mM H_2O_2, 0.1 mM ascorbic acid (AA), 0.1 mM acetaminophen (AP), 0.1 mM uric acid (UA), and 0.5 mM H_2O_2 in 10 mL of 0.1 M PBS (pH 7.0) at the applied potential of −50 mV. As shown in Fig. 7a, the response current increased obviously after addition of H_2O_2, and no obvious changed after the addition of AA, AP, and UA respectively, while the current obviously increased again after H_2O_2 was second added, indicating Nafion/Pt NPs/RGO/GC electrode showed good selectivity toward H_2O_2 and the responses caused by AA, AP and UA could be negligible. The reproducibility was assessed by detecting the responses to 0.5 mM H_2O_2 at five electrodes independently, and the relative standard deviation was calculated to 3.2%. Furthermore, the long-term stability of the prepared H_2O_2 sensor was also evaluated by measuring the response current to 0.5 mM H_2O_2 solution every day for 1 month. The electrode remained 90.6% of its initial current response for H_2O_2 after 1 month (Fig. 7b). Thus, these results indicated the prepared H_2O_2 sensor exhibited an acceptable reproducibility and long-term stability.

Real sample analysis

In order to evaluate the practical applications of the prepared non-enzymatic H_2O_2 sensor, the Nafion/Pt NPs/RGO/GC electrode was investigated to detect H_2O_2 in disinfected fetal bovine serum (FBS). As shown in Table 2, the recovery was in the range of 95.00–105.00% and RSD ranged from 3.29 to 4.12%, indicating that the H_2O_2 sensor developed in this work showed potential applicability to real samples analysis.

Conclusion

In summary, we have developed a facile and effective route to prepare prepared non-enzymatic H_2O_2 sensor based on Nafion/Pt NPs/RGO nanocomposite via one-pot method. Since Nafion is composed of mainly hydrophobic and hydrophilic chains, it could be used as stabilizer to effectively disperse RGO/Pt NPs hybrids in aqueous solution. As a sensor, the data obtained from the electrochemical experiments showed that the performances of the fabricated sensor were suitable for quantitative detection of H_2O_2 with high sensitivity, wide linear range, and low detection limit, which were much better than many other H_2O_2 sensors previously

Table 2 Determination of H_2O_2 concentration in FBS samples (n = 6)

Sample	H_2O_2 added (mM)	H_2O_2 found (mM)	Recovery (%)	R.S.D. (%)
1	0.20	0.21	105.00	3.41
2	0.40	0.38	95.00	3.29
3	0.60	0.61	101.67	4.12
4	0.80	0.81	101.25	3.67
5	1.00	0.99	99.00	3.89

reported. Furthermore, the prepared non-enzymatic H_2O_2 sensor could be also used in the detection of H_2O_2 in disinfected fetal bovine serum with an acceptable RSD. With simple synthetic method, using of low-cost materials, and excellent electrocatalytic activity, there is no doubt that Nafion/Pt NPs/RGO nanocomposite has broad prospect in fabricating high performance sensors.

Acknowledgements This work is supported by the Natural Science Foundation of China (Grant Nos. 81127001 and 81273993).

References

1. Alpat Ş, Alpat SK, Dursun Z, Telefoncu A (2009) Development of a new biosensor for mediatorless voltammetric determination of hydrogen peroxide and its application in milk samples. J Appl Electrochem 39:971–977
2. Han Y, Zheng J, Dong S (2013) A novel nonenzymatic hydrogen peroxide sensor based on Ag–MnO_2–MWCNTs nanocomposites. Electrochim Acta 90:35–43
3. Çubuk S, Yetimoğlu EK, Kahraman MV, Demirbilek P, Fırlak M (2013) Development of photopolymerized fluorescence sensor for glucose analysis. Sensors Actuators B Chem 181:187–193
4. Hanaoka S, Lin J, Yamada M (2001) Chemiluminescent flow sensor for H_2O_2 based on the decomposition of H_2O_2 catalyzed by cobalt (II)-ethanolamine complex immobilized on resin. Anal Chim Acta 426:57–64
5. Hoshino M, Kamino S, Doi M, Takada S, Mitani S, Yanagihara R, Asano M, Yamaguchi T, Fujita Y (2014) Spectrophotometric determination of hydrogen peroxide with osmium (VIII) and m-carboxyphenylfluorone. Spectrochim Acta A Mol Biomol Spectrosc 117:814–816
6. Grembecka M, Lebiedzińska A, Szefer P (2014) Simultaneous separation and determination of erythritol, xylitol, sorbitol, mannitol, maltitol, fructose, glucose, sucrose and maltose in food products by high performance liquid chromatography coupled to charged aerosol detector. Microchem J 117:77–82
7. Zakaria A, Leszczynska D (2016) Novel design of non-enzymatic sensor for rapid monitoring of hydrogen peroxide in water matrix. J Electroanal Chem 766:30–36
8. Liu W, Zhang H, Yang B, Li Z, Lei L, Zhang X (2015) A non-enzymatic hydrogen peroxide sensor based on vertical NiO nanosheets supported on the graphite sheet. J Electroanal Chem 749:62–67
9. Abdelwahab AA, Shim Y (2014) Nonenzymatic H_2O_2 sensing based on silver nanoparticles capped polyterthiophene/MWCNT nanocomposite. Sensors Actuators B Chem 201:51–58
10. Zhang Y, Zhang C, Zhang D, Ma M, Wang W, Chen Q (2016) Nano-assemblies consisting of Pd/Pt nanodendrites and poly (diallyldimethylammonium chloride)-coated reduced graphene oxide on glassy carbon electrode for hydrogen peroxide sensors. Mater Sci Eng C 58:1246–1254
11. Qi C, Zheng J (2015) Novel nonenzymatic hydrogen peroxide sensor based on Fe_3O_4/PPy/Ag nanocomposites. J Electroanal Chem 747:53–58
12. Zhang Y, Li Y, Jiang Y, Li Y, Li S (2016) The synthesis of Au@ C@ Pt core-double shell nanocomposite and its application in enzyme-free hydrogen peroxide sensing. Appl Surf Sci 378:375–383
13. Liu Y, Liu Y, Feng H, Wu Y, Joshi L, Zeng X, Li J (2012) Layer-by-layer assembly of chemical reduced graphene and carbon nanotubes for sensitive electrochemical immunoassay. Biosens Bioelectron 35:63–68
14. Zhang H, Lv X, Li Y, Wang Y, Li J (2009) P25-graphene composite as a high performance photocatalyst. ACS Nano 4:380–386
15. Chen D, Feng H, Li J (2012) Graphene oxide: preparation, functionalization, and electrochemical applications. Chem Rev 112:6027–6053
16. Wang Q, Wang Q, Li M, Szunerits S, Boukherroub R (2016) One-step synthesis of Au nanoparticle–graphene composites using tyrosine: electrocatalytic and catalytic properties. New J Chem 40: 5473–5482
17. Kim KS, Zhao Y, Jang H, Lee SY, Kim JM, Kim KS, Ahn J, Kim P, Choi J, Hong BH (2009) Large-scale pattern growth of graphene films for stretchable transparent electrodes. Nature 457:706–710
18. Xu C, Wang X, Zhu J (2008) Graphene–metal particle nanocomposites. J Phys Chem C 112:19841–19845
19. Yang Z, Zheng Q, Qiu H, Jing LI, Yang J (2015) A simple method for the reduction of graphene oxide by sodium borohydride with $CaCl_2$ as a catalyst. New Carbon Mater 30:41–47
20. Yin H, Zhou Y, Ma Q, Ai S, Ju P, Zhu L, Lu L (2010) Electrochemical oxidation behavior of guanine and adenine on graphene–Nafion composite film modified glassy carbon electrode and the simultaneous determination. Process Biochem 45:1707–1712
21. Choi BG, Im J, Kim HS, Park H (2011) Flow-injection amperometric glucose biosensors based on graphene/Nafion hybrid electrodes. Electrochim Acta 56:9721–9726
22. Zhang J, Gao L, Sun J, Liu Y, Wang Y, Wang J, Kajiura H, Li Y, Noda K (2008) Dispersion of single-walled carbon nanotubes by nafion in water/ethanol for preparing transparent conducting films. J Phys Chem C 112:16370–16376
23. Singh AS, Shendage SS, Nagarkar JM (2014) Electrochemical synthesis of copper nanoparticles on nafion–graphene nanoribbons and its application for the synthesis of diaryl ethers. Tetrahedron Lett 55: 4917–4922
24. Er E, Çelikkan H, Erk N, Aksu ML (2015) A new generation electrochemical sensor based on graphene nanosheets/gold nanoparticles/nafion nanocomposite for determination of Silodosin. Electrochim Acta 157:252–257
25. Niu X, Chen C, Zhao H, Chai Y, Lan M (2012) Novel snowflake-like Pt–Pd bimetallic clusters on screen-printed gold nanofilm electrode for H_2O_2 and glucose sensing. Biosens Bioelectron 36:262–266
26. Mei H, Wu W, Yu B, Wu H, Wang S, Xia Q (2016) Nonenzymatic electrochemical sensor based on Fe@ Pt core–shell nanoparticles for hydrogen peroxide, glucose and formaldehyde. Sensors Actuators B Chem 223:68–75
27. Zhang J, Li J, Yang F, Zhang B, Yang X (2010) Pt nanoparticles-assisted electroless deposition of Prussian blue on the electrode: detection of H_2O_2 with tunable sensitivity. J Electroanal Chem 638:173–177
28. Fang Y, Zhang D, Qin X, Miao Z, Takahashi S, Anzai J, Chen Q (2012) A non-enzymatic hydrogen peroxide sensor based on poly (vinyl alcohol)–multiwalled carbon nanotubes–platinum nanoparticles hybrids modified glassy carbon electrode. Electrochim Acta 70:266–271
29. Si Y, Samulski ET (2008) Exfoliated graphene separated by platinum nanoparticles. Chem Mater 20:6792–6797
30. Xing Y (2004) Synthesis and electrochemical characterization of uniformly-dispersed high loading Pt nanoparticles on sonochemically-treated carbon nanotubes. J Phys Chem B 108: 19255–19259
31. Zhang C, Zhang Y, Miao Z, Ma M, Du X, Lin J, Han B, Takahashi S, Anzai J, Chen Q (2016) Dual-function amperometric sensors based on poly (diallydimethylammoniun chloride)-functionalized

reduced graphene oxide/manganese dioxide/gold nanoparticles nanocomposite. Sensors Actuators B Chem 222:663–673
32. Niu Z, Chen J, Hng HH, Ma J, Chen X (2012) A leavening strategy to prepare reduced graphene oxide foams. Adv Mater 24:4144–4150
33. Ketpang K, Son B, Lee D, Shanmugam S (2015) Porous zirconium oxide nanotube modified Nafion composite membrane for polymer electrolyte membrane fuel cells operated under dry conditions. J Membrane Sci 488:154–165
34. Zhang D, Fang Y, Miao Z, Ma M, Du X, Takahashi S, Anzai J, Chen Q (2013) Direct electrodeposion of reduced graphene oxide and dendritic copper nanoclusters on glassy carbon electrode for electrochemical detection of nitrite. Electrochim Acta 107:656–663
35. Guan Y, Dai M, Liu T, Liu Y, Liu F, Liang X, Suo H, Sun P, Lu G (2016) Effect of the dispersants on the performance of fuel cell type CO sensor with Pt–C/Nafion electrodes. Sensors Actuators B Chem 230:61–69
36. Ensafi AA, Jafari-Asl M, Rezaei B (2014) A new strategy for the synthesis of 3-D Pt nanoparticles on reduced graphene oxide through surface functionalization, application for methanol oxidation and oxygen reduction. Electrochim Acta 130:397–405
37. Du X, Miao Z, Zhang D, Fang Y, Ma M, Chen Q (2014) Facile synthesis of β-lactoglobulin-functionalized multi-wall carbon nanotubes and gold nanoparticles on glassy carbon electrode for electrochemical sensing. Biosens Bioelectron 62:73–78
38. Bian X, Lu X, Jin E, Kong L, Zhang W, Wang C (2010) Fabrication of Pt/polypyrrole hybrid hollow microspheres and their application in electrochemical biosensing towards hydrogen peroxide. Talanta 81:813–818
39. Fang K, Yang Y, Fu L, Zheng H, Yuan J, Niu L (2014) Highly selective H_2O_2 sensor based on 1-D nanoporous Pt@ C hybrids with core–shell structure. Sensors Actuators B Chem 191:401–407
40. Cui X, Li Z, Yang Y, Zhang W, Wang Q (2008) Low-potential sensitive hydrogen peroxide detection based on nanotubular TiO_2 and platinum composite electrode. Electroanalysis 20:970–975
41. Sun Y, He K, Zhang Z, Zhou A, Duan H (2015) Real-time electrochemical detection of hydrogen peroxide secretion in live cells by Pt nanoparticles decorated graphene–carbon nanotube hybrid paper electrode. Biosens Bioelectron 68:358–364
42. Xu F, Sun Y, Zhang Y, Shi Y, Wen Z, Li Z (2011) Graphene–Pt nanocomposite for nonenzymatic detection of hydrogen peroxide with enhanced sensitivity. Electrochem Commun 13:1131–1134
43. Zhai D, Liu B, Shi Y, Pan L, Wang Y, Li W, Zhang R, Yu G (2013) Highly sensitive glucose sensor based on Pt nanoparticle/polyaniline hydrogel heterostructures. ACS Nano 7:3540–3546
44. Xu L, Zhu Y, Tang L, Yang X, Li C (2008) Dendrimer-encapsulated Pt nanoparticles/polyaniline nanofibers for glucose detection. J Appl Polym Sci 109:1802–1807